Journal of Applied Pharmaceutical Science Vol. 11(07), pp 163-171, July, 2021
Available online at http://www.japsonline.com
DOI: 10.7324/JAPS.2021.110719
ISSN 2231-3354

# Identification of the volatile and nonvolatile constituents of *Schinus molle* (L.) fruit extracts and estimation of their activities as anticancer agents

Ezzat E. A. Osman[1*], Eman A. Morsi[1], Mortada M. El-Sayed[1], Adil Gobouri[2], El-Sayed S. Abdel-Hameed[1]

[1]Medicinal Chemistry Laboratory, Theodor Bilharz Research Institute, Giza, Egypt.
[2]Chemistry Department, Faculty of Science, Taif University, Taif, Kingdom of Saudi Arabia.

**ARTICLE INFO**

Received on: 28/03/2021
Accepted on: 23/04/2021
Available online: 05/07/2021

***Key words:***
Anticancer, flavonoids, GC-MS, LC-ESI-MS, phenolic, *Schinus molle.*

**ABSTRACT**

This work was designed to assess the cytotoxic potential of *Schinus molle* (L.) fruit extracts and characterization of their chemical composition. The cytotoxicity of *S. molle* extracts was carried out on hepatoma HepG2 cell line using the Sulforhodamine B method. The volatile constituents of *S. molle* normal-hexane (*n*-hexane) extract and the essential oil were identified by gas chromatography-mass spectrometry (GC-MS), whereas the nonvolatile chemical compositions were investigated using the Liquid chromatography-electron spray ionization-mass spectrometry (LC-ESI-MS) technique. The *n*-hexane extract showed the highest cytotoxic inhibition activity on the HepG2 cell line in a concentration-dependent manner with inhibition concentration ($IC_{50}$ = 9.75 µg/ml), followed by *n*-butanol fraction ($IC_{50}$ = 10.70 µg/ml) and the essential oil ($IC_{50}$ = 11.90 µg/ml). The GC-MS investigation of the essential oil afforded 50 compounds classified into monoterpenes and sesquiterpenes with different percentiles. The most abundant monoterpenes were α-phellandrene, myrcene, D-limonene, β-phellandrene, and α-pinene. At the same time, the major sesquiterpenes were juniper camphor, guaiyl acetate, γ-gurjunene, α-cadinol, and β-caryophyllene. On the other hand, the LC-ESI-MS investigation of the methanolic extract, *n*-butanol fraction, and aqueous part led to the identification of 31 phenolic compounds classified as phenolic acids, phenylethanoids, flavonoids, and tannins. These findings demonstrate the remarkable potentiality of *S. molle* extracts as a valuable source of anticancer capacity.

## INTRODUCTION

Cancer is a prevalent disease which is considered as the second leading cause of mortality across the globe and the number of new cases increases day per day, especially in Asia, Africa, and USA (Nguyen *et al*., 2020; Singh and Patra, 2018). Cancer is a public health problem in developed and developing countries that affects human health and economic conditions (Shahat *et al*., 2019). Among cancers, hepatocellular carcinoma (HCC) or liver cancer is the primary virulent tumor and the most common type of cancer that arises from the parenchymal liver cells. It is considered as the third leading reason for cancer deaths after lung and stomach cancers (Bray *et al*., 2018). Also, it represents the seventh cancer infection in women and the fifth in men (Anyasor *et al*., 2020). The main risk factors for HCC include nonalcoholic fatty liver disease, hepatitis C and B viral infections, alcoholism, diabetes, obesity, primary biliary cirrhosis, and exposure to nitrosamines and aflatoxins (Abdel-Hamid *et al*., 2018; Chedid *et al*., 2017). The most popular treatment strategies of HCC are chemoembolization, orthotopic liver transplantation, and chemotherapy. The chemotherapy treatment protocol is the preferred method for advanced hepatocellular carcinoma. Unfortunately, chemotherapy is associated with drug resistance and other side effects that lead to liver failure (Siddiqui *et al*., 2019). On the other hand, the effective and safe alternative therapeutic tools for the treatment of HCC were natural products, especially secondary metabolites (Huang *et al*., 2016). Plant secondary metabolites are used in the health care system since ancient times. More than thousands of medicinal plants have been identified to possess many medicinal

*Corresponding Author
*Ezzat E. A. Osman, Medicinal Chemistry Laboratory, Theodor Bilharz Research Institute, Giza, Egypt. E-mail: ezzat_ea @ yahoo.com*

and pharmacological properties, including anticancer agents (Khlifi *et al*., 2013).

*Schinus molle* (L.), or pepper tree, belongs to the family Anacardiaceae comprising 72 genera and 600 species (Machado *et al*., 2019). *Schinus molle* is growing in tropical and subtropical areas worldwide including South America and Mediterranean countries (Malca-García *et al*., 2017). *Schinus molle* has high amounts of oil with a spicy smell which is used in the food industry, ornamentals, and medicines (Garzoli *et al*., 2019). In folklore medicine, the extracts of *S. molle* were documented as antitumor, astringent, antiviral, antioxidant, antimicrobial, anti-inflammatory, digestive stimulant, diuretic, and wound healer activities (Gomes *et al*., 2013; Hosni *et al*., 2011; López *et al*., 2014; Malca-García *et al*., 2017; Martins *et al*., 2014). The previously chemical investigation studies of *S. molle* have been reported; it contains various chemical ingredients, including monoterpenoid, sesquiterpenoid, triterpenoids, tannins, and flavonoids (Abdel-Hameed and Bazaid, 2017; Ono *et al*., 2008). To the best of our knowledge, there were no reports on the chemical investigation of *S. molle* fruits growing in Taif City, Saudi Arabia.

The main objectives of this work were (i) extraction of volatile and nonvolatile chemical components of *S. molle* fruits, (ii) investigation of the anticancer potential of different extracts of *S. molle* fruits, (iii) characterization of the chemical composition of *S. molle* fruits essential oil and *n*-hexane extract using gas chromatography-mass spectrometry (GC-MS) analysis, and (iv) identification of the nonvolatile chemical constituents using Liquid chromatography-electron spray ionization-mass spectrometry (LC-ESI-MS) analysis.

## MATERIALS AND METHODS

### Plant materials

The mature fruits of *S. molle* were collected from Taif city, Saudi Arabia. The plant sample was authenticated by Dr. Mohamed Fadle, Professor of Plant Taxonomy, Faculty of Science, Taif University, Taif, Saudi Arabia. A voucher specimen (no. 13518) of plant fruits was deposited in the Medicinal Chemistry laboratory, Theodor Bilharz Research Institute, Giza, Egypt. The fresh fruits were crushed using an electric mill to be ready for the extraction process.

### Extraction of essential oil

150 g of freshly crushed fruits of *S. mole* was mixed with 2 l of distilled $H_2O$ in a round flask and hydrodistillated at 90°C using the Clevenger instrument. The system was operated till the essential oil was limited. 9.2 ml of the essential oil was collected and dried over anhydrous sodium sulfate. The obtained essential oil was stored at −20°C in a glass vial and away from contamination for biological and chemical investigations.

### Preparation of organic extracts

150 g of freshly crushed fruits of *S. mole* was immersed in 750 ml *n*-hexane for 7 days at room temperature and then filtered using filter paper (Whatman No. 1). The *n*-hexane solvent was removed using a rotary evaporator (BUCHI, Switzerland) under reduced pressure and the extraction process was repeated three times. 12.3 ml yellow turbid viscous oily *n*-hexane extract was obtained. After extraction with *n*-hexane, the residue was extracted with 750 ml 85% Methanol (MeOH). The solvent was evaporated under vacuum to give a 30.7 g solid brown extract. Furthermore, 20 g of 85% MeOH extract (MeOH ext.) was dissolved in 100 ml distilled $H_2O$ and partitioned with normal-butanol (*n*-BuOH) (3 × 100 ml solvent) using a separating funnel. The *n*-BuOH and aqueous layers were separated and evaporated under reduced pressure to afford 8.3 g of *n*-BuOH fraction and 11.1 g of aqueous part. All extracts were kept in glass bottles for chemical profiling and biological investigations.

### Cytotoxicity studies

The samples under the current study were *in vitro* tested against human liver carcinoma (HepG2) cell line, which was carried out at the National Cancer Institute, Cairo, Egypt, according to Skehan *et al*.'s (1990) method. Briefly, the HepG2 cells were seeded in 96-well microplates at a conc. ($5 \times 10^4 - 10^5$ cell/well) in a fresh medium and left for 24 hours. The samples (100 µl) with different concentrations (0.0, 12.5, 25, 50, and 100 µg/ml) have been added to the wells. The microplate wells' total volume was completed up to 200 (µl volume/well) using a fresh medium and then incubated for 48 hours in 5% $CO_2$ incubator at a temperature of 37°C. After 48 hours, the cells were fixed with 50 µl trichloroacetic acids (cold 50%) for 1 hour at 4°C. Moreover, the wells were washed with distilled $H_2O$ (5 times) and stained for 30 minutes at room temperature by 50 µl Sulforhodamine B (SRB) (0.4%). Furthermore, the plate wells were washed four times using acetic acid (1%), the plates were dried carefully, and then the dye was solubilized in 10 mM tris base at pH 10.5 (100 µl/well) for 5 minutes at 1,600 rpm using a shaker (Orbital Shaker OS 20, Boeco, Germany). The optical density of plate wells was determined by a spectrophotometer at 564 nm with ELIZA microplate reader (Meter tech. Σ 960, USA). Doxorubicin was used as a standard and the experiment was repeated in triplicate. The cell viability (%) was calculated from the following equation:

The cell viability (%) = [Optical density of treated cells/Optical density control cells] × 100.

In addition, $IC_{50}$ was calculated from the cell viability curve of the cancer cell lines.

### GC-MS conditions

The essential oil and *n*-hexane extract volatile chemical composition were investigated using gas chromatograph CP 3800 interfaced with a Saturn 2200 mass spectrometer (Varian, California, USA) with electron impact ionization (70 eV). A VF-5 fused silica capillary column (30 m × 0.25 mm, 0.25 µm film thickness) was used. The carrier gas was helium with a constant flow rate (1 ml/minute). The temperature of the oven was adjusted for 1 minute at 50°C, increased gradually to 120°C (5°C/minutes), 120°C–190°C (2°C/minutes), held for 1 minute at 190°C, 190°C–250°C (10°C/minutes), and held for 3 minutes at 260°C. The mass range of recorded ions was 45–400 *m/z* and the total run time was 60 minutes. The injected samples and standard mixture (1 mg/1 ml *n*-hexane) were prepared. The samples and standards (1 µl) were injected by autosampler with a split ratio of 1:20. The volatile constituents were characterized by cob 1qmparison

of their retention time ($t_R$), retention indices relative to ($C_8$–$C_{20}$) *n*-alkanes with standards, and matching their mass spectra with corresponding data (Wiley and NIST electronic libraries).

### LC-ESI-MS conditions

A sample solution (5 mg/ml) of 85% MeOH ext., *n*-BuOH fraction, and aqueous part of *S. molle* fruits was prepared by a mixture of $CH_3CN$:MeOH:$H_2O$ (1:1:2; *v/v/v*) and then filtered by 0.45 µm Nylon filter disk for injection to LC-ESI-MS system. The LC system (Waters Alliance 2695, Waters, USA) containing a reversed-phase column (RP-C18 Phenomenex 250 mm with 5 $\mu$m particle size) is hyphenated with a mass analyzer (Waters 3100). The LC mobile phase was filtered and degassed well, and analysis was carried out using gradient mobile phase with a flow rate (0.4 ml/minutes). The mobile phase consists of two eluents, mobile phase A ($H_2O$ containing 0.1% formic acid), and mobile phase B ($CH_3CN$:MeOH; 1:1 and acidified with 0.1% formic acid). The LC time program was carried out as follows: 0–5 minutes (5% B); 5–10 minutes (5%–10% B); 10–55 minutes (10%–50% B); 55–65 minutes (50%–95% B); 65–70 minutes (5% B). The injected sample volume was 20 $\mu$l and analysis was performed in negative ion mode (in range *m/z* 50–1,000) with the following parameters: cone voltage (50 eV), capillary voltage (3 kV), source temperature (150°C), desolvation temperature (350°C), desolvation gas flow (600 l/hours), and cone gas flow (50 l/hours). The compound peaks were analyzed using software (Maslynx 4.1) and tentatively identified by comparing their mass spectra fragmentation pattern and retention time with standards and published data.

### Data analysis

The data analysis was performed by the SPSS software for Windows (version 13.0) and all data were expressed as mean ± standard deviation.

## RESULTS AND DISCUSSION

### Cytotoxic activity

The cytotoxic activity of the *S. molle* different extracts such as the essential oil, 85% MeOH ext., *n*-hexane extract, *n*-BuOH fraction, and aqueous part was assayed against HepG2 cell line using SRB colorimetric assay. This assay exhibits the ability of SRB to attach with protein components of the cells, which are fixed by trichloroacetic acid to the tissue culture plates (Vichai and Kirtikara, 2016). Figure 1 exhibited the cell viability of *S. molle* fruit extracts, which represented the 85% extract had the highest cell viability, followed by the aqueous part, essential oil, *n*-BuOH fr., and *n*-hexane extract. On the other hand, it showed the $IC_{50}$ value of *S. molle* fruit extracts and doxorubicin as a broad-spectrum anticancer drug. The results in Figure 2 showed that *n*-hexane ext. and *n*-BuOH fr. of *S. molle* exhibited the highest anticancer activity ($IC_{50}$ = 9.75 and 10.70 µg/ml, respectively), followed by essential oil ($IC_{50}$ = 11.90 µg/ml), aqueous part ($IC_{50}$ = 15.80 µg/ml), and 85% MeOH ext. ($IC_{50}$ = 16.40 µg/ml). The cytotoxic evaluation criteria of the plant extracts are according to American National Cancer Institute (NCI) protocols, in which the cytotoxic evaluation criteria of the plant extracts were considered to be significant when the $IC_{50}$ values ≤ 30 (µg/ml), while for pure substances, the $IC_{50}$ values should be ≤ 4 µg/ml (Geran *et al*., 1972). Therefore, all *S. molle* fruit extracts were considered to be significant anticancer plant extracts against HepG2 cell line. It was clearly appeared that the cytotoxic activity of the MeOH extract in the current study ($IC_{50}$=16.40 µg/ml) had much higher cytotoxic activity than the MeOH extract of the same plant growing in Argentine ($IC_{50}$= 50 µg/ml) as reported by Hamdan *et al*., (2016). Thus, the difference in cytotoxic activity may be due to the different time of collection and climate conditions. So, it is imperative to identify both volatile and nonvolatile constituents of *S. molle* extracts to know their chemical nature.

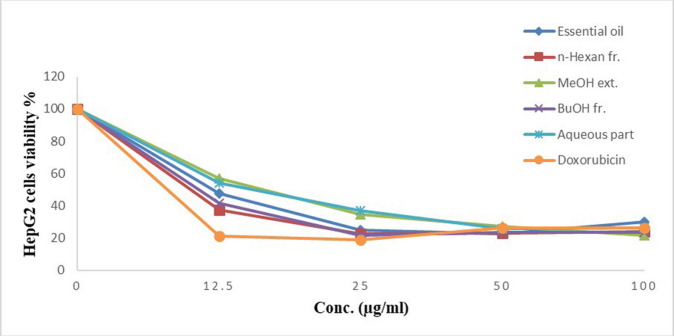


**Figure 1.** Cytotoxic activity of *S. molle* fruit extracts towards human liver carcinoma cell line (HepG-2).

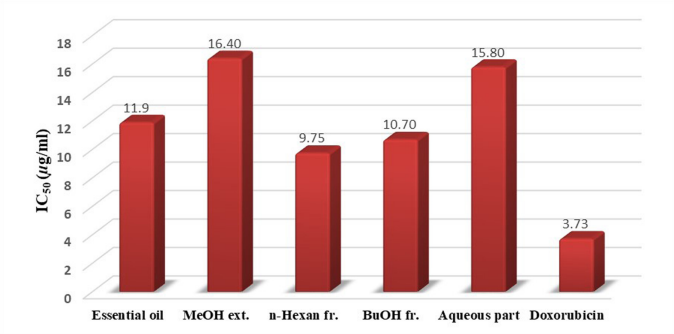


**Figure 2.** $IC_{50}$ of tested *S. molle* fruit extracts against HepG-2 cell line.

### GC-MS investigation of *S. molle* fruits n-hexane extract and the essential oil

The GC-MS investigation of *S. molle* *n*-hexane extract and essential oil (Table 1 and Fig. 3) characterizes 50 compounds in both extracts with different percentages, corresponding to 99.46% in essential oil and 98.59% for *n*-hexane ext., in which 17 compounds of them were higher than 1% relative to the total volatile composition of *S. molle* fruits essential oil and *n*-hexane ext. The highest amount of monoterpenes (67.81%) was detected in essential oil, whereas *n*-hexane ext. had 37.87% of the total components. The main identified monoterpenes were α-phellandrene (26.24% in the essential oil; 17.70% in *n*-hexane ext.), myrcene (21.57% in the essential oil; 12.33% in *n*-hexane ext.), D-limonene (7.93% in the essential oil; 4.84% in *n*-hexane ext.), β-phellandrene (7.28% in the essential oil; 5.33% in *n*-hexane ext.), and α-pinene (2.69% in the essential oil; 1.17% in *n*-hexane ext.). On the other hand, sesquiterpenes were detected as major components in *n*-hexane ext. (59.23%), while the essential

**Table 1.** Chemical composition of *S. molle* fruits essential oil and *n*-hexane ext.

| No. | Name | $t_R$ | RI | Essential oil % | *n*-hexane ext. % | MW | MF | Method of identification | Essential oil group |
|---|---|---|---|---|---|---|---|---|---|
| 1 | α-pinene | 7.08 | 935 | 2.69 | 1.17 | 136 | $C_{10}H_{16}$ | St, NIST, RI | Bicyclic monoterpene |
| 2 | Sabinene1 | 8.14 | 975 | 0.20 | 0.11 | 136 | $C_{10}H_{16}$ | St, NIST, RI | Bicyclic monoterpene |
| 3 | β-pinene | 8.30 | 981 | 0.29 | 0.14 | 136 | $C_{10}H_{16}$ | St, NIST, RI | Bicyclic monoterpene |
| 4 | Myrcene | 8.59 | 991 | 21.57 | 12.33 | 136 | $C_{10}H_{16}$ | St, NIST, RI | Acyclic monoterpene |
| 5 | α-phellandrene | 9.13 | 1010 | 26.24 | 12.70 | 136 | $C_{10}H_{16}$ | St, NIST, RI | Monocyclic monoterpene |
| 6 | p-cymene | 9.61 | 1028 | 0.86 | 0.46 | 134 | $C_{10}H_{14}$ | St, NIST, RI | Alkylbenzene monoterpene |
| 7 | D-limonene | 9.76 | 1032 | 7.93 | 4.84 | 136 | $C_{10}H_{16}$ | St, NIST, RI | Monocyclic monoterpene |
| 8 | β-phellandrene | 9.82 | 1035 | 7.28 | 5.33 | 136 | $C_{10}H_{16}$ | NIST, RI | Monocyclic monoterpene |
| 9 | α-terpinolene | 11.36 | 1089 | 0.24 | 0.16 | 136 | $C_{10}H_{16}$ | St, NIST, RI | Monocyclic monoterpene |
| 10 | Linalool | 11.74 | 1102 | 0.16 | 0.08 | 154 | $C_{10}H_{18}O$ | St, NIST, RI | Acyclic monoterpene |
| 11 | Octanoic acid, methyl ester | 12.40 | 1125 | 1.92 | 1.44 | 158 | $C_9H_{18}O_2$ | NIST, RI | Fatty acid methy ester |
| 12 | Nonanoic acid, methyl ester | 14.37 | 1194 | 0.11 | 0.05 | 156 | $C_{10}H_{20}O$ | NIST, RI | Fatty acid methy ester |
| 13 | Carvacrol | 17.45 | 1294 | 0.17 | 0.24 | 150 | $C_{10}H_{14}O$ | NIST, RI | Monocyclic monoterpene phenol |
| 14 | α-cubebene | 19.44 | 1348 | 0.25 | 0.34 | 204 | $C_{15}H_{24}$ | NIST, RI | Tricyclic sesquiterpene |
| 15 | Neryl acetate | 19.79 | 1357 | 0.18 | 0.31 | 196 | $C_{12}H_{20}O_2$ | St, NIST, RI | Acyclic monoterpene |
| 16 | α-copaene | 20.56 | 1388 | 0.24 | 0.28 | 204 | $C_{15}H_{24}$ | NIST, RI | Tricyclic sesquiterpene |
| 17 | β-elemene | 21.07 | 1392 | 0.19 | 0.11 | 204 | $C_{15}H_{24}$ | NIST, RI | Monocyclic sesquiterpene |
| 18 | α-gurjunene | 21.82 | 1410 | 0.78 | 0.92 | 204 | $C_{15}H_{24}$ | NIST, RI | Tricyclic sesquiterpene |
| 19 | β- caryophyllene | 22.35 | 1422 | 2.56 | 3.29 | 204 | $C_{15}H_{24}$ | St, NIST, RI | Bicyclic sesquiterpene |
| 20 | (+)-Aromadendrene | 23.12 | 1441 | 0.33 | 0.12 | 204 | $C_{15}H_{24}$ | NIST, RI | Tricyclic sesquiterpene |
| 21 | Z-β-Farnesene | 23.67 | 1453 | 0.19 | 0.28 | 204 | $C_{15}H_{24}$ | NIST, RI | sesquiterpene |
| 22 | α-humulene | 23.85 | 1457 | 0.69 | 1.04 | 204 | $C_{15}H_{24}$ | NIST, RI | Monocyclic sesquiterpene |
| 23 | (-)-Allo-aromadendrene | 24.04 | 1462 | 0.43 | 0.58 | 204 | $C_{15}H_{24}$ | NIST, RI | Tricyclic sesquiterpene |
| 24 | α-cadinene | 24.54 | 1473 | 0.14 | 0.08 | 204 | $C_{15}H_{24}$ | NIST, RI | Bicyclic sesquiterpene |
| 25 | β-cadinene | 24.67 | 1476 | 0.26 | 0.12 | 204 | $C_{15}H_{24}$ | NIST, RI | Bicyclic sesquiterpene |
| 26 | β-cubebene | 24.95 | 1483 | 0.22 | 0.27 | 204 | $C_{15}H_{24}$ | NIST, RI | Tricyclic sesquiterpene |
| 27 | Valencene | 25.05 | 1485 | 0.08 | 0.13 | 204 | $C_{15}H_{24}$ | NIST, RI | Bicyclic sesquiterpene |
| 28 | α-guaiene | 25.31 | 1491 | 0.28 | 0.36 | 204 | $C_{15}H_{24}$ | NIST, RI | Bicyclic sesquiterpene |
| 29 | (+)-Epi-bicyclosesquiphellandrene | 25.42 | 1494 | 0.35 | 0.15 | 204 | $C_{15}H_{24}$ | NIST, RI | Bicyclic sesquiterpene |
| 30 | γ-gurjunene | 25.63 | 1499 | 7.51 | 10.51 | 204 | $C_{15}H_{24}$ | NIST, RI | Bicyclic sesquiterpene |
| 31 | α-muurolene | 25.73 | 1501 | 0.19 | 0.16 | 204 | $C_{15}H_{24}$ | NIST, RI | Bicyclic sesquiterpene |
| 32 | D-longifolene | 26.13 | 1509 | 1.00 | 1.65 | 204 | $C_{15}H_{24}$ | NIST, RI | Tricyclic sesquiterpene |
| 33 | γ-cadinene | 26.39 | 1515 | 0.92 | 0.06 | 204 | $C_{15}H_{24}$ | NIST, RI | Bicyclic sesquiterpene |
| 34 | δ-Cadinene | 26.62 | 1519 | 4.63 | 1.51 | 204 | $C_{15}H_{24}$ | NIST, RI | Bicyclic sesquiterpene |
| 35 | Cadina-1,4-diene | 27.25 | 1533 | 0.18 | 0.17 | 204 | $C_{15}H_{24}$ | NIST, RI | Bicyclic sesquiterpene |
| 36 | Isoledene | 27.46 | 1538 | 0.15 | 0.06 | 204 | $C_{15}H_{24}$ | NIST, RI | Tricyclic sesquiterpene |
| 37 | α-himachalene | 27.60 | 1540 | 0.36 | 0.54 | 204 | $C_{15}H_{24}$ | NIST, RI | Bicyclic sesquiterpene |
| 38 | (-)-caryophyllene(II) | 28.00 | 1549 | 0.28 | 0.43 | 204 | $C_{15}H_{24}$ | NIST, RI | Bicyclic sesquiterpene |
| 39 | Palustrol | 29.03 | 1571 | 0.24 | 0.45 | 222 | $C_{15}H_{26}O$ | NIST, RI | Tricyclic sesquiterpene alcohol |
| 40 | α-cadinol | 29.32 | 1577 | 1.40 | 4.01 | 222 | $C_{15}H_{26}O$ | NIST, RI | Bicyclic sesquiterpene alcohol |
| 41 | α-eudesmol | 30.18 | 1595 | 0.53 | 1.17 | 222 | $C_{15}H_{26}O$ | NIST, RI | Bicyclic sesquiterpene alcohol |
| 42 | Viridiflorol | 30.67 | 1605 | 0.20 | 0.60 | 222 | $C_{15}H_{26}O$ | NIST, RI | Tricyclic sesquiterpene alcohol |
| 43 | β-cadinol | 31.98 | 1633 | 0.16 | 0.25 | 222 | $C_{15}H_{26}O$ | NIST, RI | Bicyclic sesquiterpene alcohol |
| 44 | t-cadinol | 32.46 | 1643 | 0.35 | 0.14 | 222 | $C_{15}H_{26}O$ | NIST, RI | Bicyclic sesquiterpene alcohol |
| 45 | t-muurolol | 32.56 | 1644 | 0.53 | 0.12 | 222 | $C_{15}H_{26}O$ | NIST, RI | Bicyclic sesquiterpene alcohol |
| 46 | Guaiol | 33.11 | 1655 | 1.10 | 0.88 | 222 | $C_{15}H_{26}O$ | NIST, RI | Bicyclic sesquiterpene alcohol |
| 47 | γ-eudesmol | 33.96 | 1673 | 0.08 | 1.06 | 222 | $C_{15}H_{26}O$ | NIST, RI | Bicyclic sesquiterpene alcohol |
| 48 | Juniper camphor | 34.95 | 1694 | 1.60 | 14.01 | 222 | $C_{15}H_{26}O$ | NIST, RI | Bicyclic sesquiterpene alcohol |

*(Continued)*

| No. | Name | $t_R$ | RI | Essential oil % | *n*-hexane ext. % | MW | MF | Method of identification | Essential oil group |
|---|---|---|---|---|---|---|---|---|---|
| 49 | Eudesma-4(14),11-diene | 35.78 | 1710 | 0.06 | 0.15 | 204 | $C_{15}H_{24}$ | NIST, RI | Bicyclic sesquiterpene |
| 50 | Guaiyl acetate | 38.62 | 1768 | 1.16 | 13.23 | 264 | $C_{17}H_{28}O_2$ | NIST, RI | Bicyclic sesquiterpene acetate |
| | Compounds identified compounds | | | 99.46 | 98.59 | | | | |
| | Monoterpenes hydrocarbons | | | 67.30 | 37.24 | | | | |
| | Oxygenated monoterpenes | | | 0.51 | 0.63 | | | | |
| | Total monoterpenes | | | 67.81 | 37.87 | | | | |
| | Sesquiterpenes hydrocarbons | | | 22.21 | 23.16 | | | | |
| | Oxygenated sesquiterpenes | | | 7.41 | 36.07 | | | | |
| | Total sesquiterpenes | | | 29.62 | 59.23 | | | | |
| | Fatty acid derivatives | | | 2.03 | 1.49 | | | | |

$t_R$ = retention time; RI = retention indices; MW = Molecular weight; MF = Molecular formula.

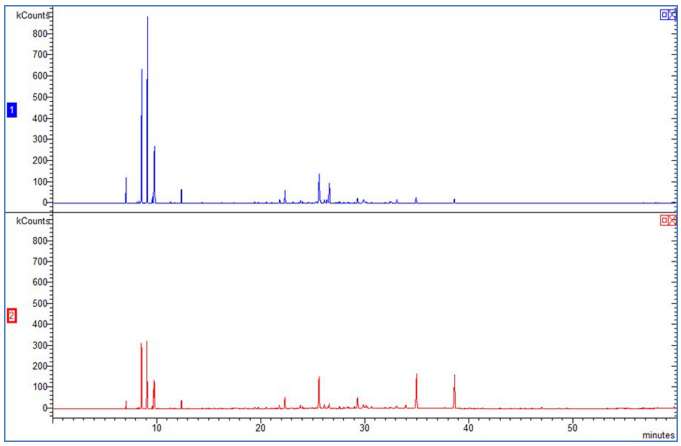


**Figure 3.** GC-MS chromatograms of *S. molle* fruit essential oil (1) and *n*-hexane extract (2).

oil had 29.62% sesquiterpenes of the total components. Among them, juniper camphor (14.01% in *n*-hexane ext. and 1.60% in essential oil), guaiyl acetate (13.23% in *n*-hexane ext. and 1.16% in essential oil), γ-gurjunene (10.51% in *n*-hexane ext. and 7.51% in essential oil), α-cadinol (4.01% in *n*-hexane ext. and 1.40% in essential oil), and β-caryophyllene (3.29% in *n*-hexane ext. and 2.56% in essential oil) were the major identified sesquiterpenes. Some previous studies reported that *S. molle* aerial parts and fruits essential oils were riches with monoterpenes (Abdel-Sattar *et al*., 2010; Gomes *et al*., 2013; Hayouni *et al*., 2008; Machado *et al*., 2019; Martins *et al*., 2014), while some other studies reported that sesquiterpenes were represented as the main constituents (Abdel-Hameed and Bazaid, 2017; Cavalcanti *et al*., 2015; Garzoli *et al*., 2019; Simionatto *et al*., 2011). Thus, the variations in the chemical compositions percentiles of *S. molle* fruits essential oil and *n*-hexane ext. may be due to some thermal and chemical factors. Furthermore, the potent cytotoxic activity of *n*-hexane extract could be due to the presence of a high amount of monocyclic monoterpenes, acyclic monoterpenes, bicyclic monoterpenes, and bicyclic sesquiterpenes.

## LC-ESI-MS profiling of organic extracts

A total of 31 phenolic compounds were the most abundant metabolites in *S. molle* fruits extracts (85% MeOH ext., *n*-BuOH fr., and aqueous part) characterized by LC-ESI-MS investigation in negative ion mode as shown in Table 2 and Figures 4 and 5. The detected compounds were numbered by their retention time order and tentatively identified by the mass fragmentation pattern and comparison with literature.

Compound **1** (Rt = 2.92 minutes) exhibited molecular ion peak at *m/z* 391 $[M-H]^-$, gave abundant ion peak at *m/z* 195 $[M-H-196]^-$, and reflected the presence of hydroxytyrosol acetate dimer. In addition, compound **2** (Rt = 3.00 minutes) exhibited a base peak at *m/z* 357 $[M-H]^-$, afforded an abundant peak at *m/z* 195% $[M-H-162]^-$, and reflected the loss of hexoside unit. It was tentatively assigned as hydroxytyrosol acetate-hexoside (Tasioula-Margari and Tsabolatidou, 2015). As can be seen in Table 2, compound **4** (Rt = 8.09 minutes) displayed $[M-H]^-$ ion peak at *m/z* 169 and gave a fragment ion at *m/z* 125 $[M-44-H]^-$, due to the loss of carboxylic group and this fragmentation pattern is typical for gallic acid as compared with standard. (Escobar-Avello *et al*., 2019). The derivatives of gallic acid were identified in the tested extracts by comparing their retention time and mass spectra. Compound **3** (Rt = 5.84 minutes) showed a deprotonated molecule at *m/z* 331 and yielded fragment ions at *m/z* 169 $[M-162-H]^-$, which is related to the loss of hexoside moiety. Therefore, this compound was assigned as galloyl-*O*-hexoside (Mena *et al*., 2012). Compound **8** (Rt = 21.20 minutes) represents the precursor ion at *m/z* 183 $[M-H]^-$, gives another fragment at *m/z* 169 $[M-14-H]^-$, and refers to loss of the methyl group. Thus, compound **8** was assigned as methyl gallate. Compounds **5** and 6 (Rt = 15.78 and 16.78 minutes, respectively) exhibited a deprotonated peak ion $[M-H]^-$ at *m/z* 325 and afforded a signal at *m/z* 169, 125, and 79, characteristic for galloyl shikimic acid and its isomer (Wyrepkowski *et al*., 2014). Furthermore, compounds **9** and **10** (Rt = 27.80 and 28.89 minutes, respectively) displayed a deprotonated ion $[M-H]^-$ peak at *m/z* 477 and afforded fragment at *m/z* 325 $[M-152-H]^-$, which means loss of the gallic acid unit. Therefore, this compound was characterized as digalloyl shikimic acid and its isomer (Li and Seeram, 2018). Compounds **11** (Rt = 32.98 minutes) and **12** (Rt = 33.06 minutes) had the same deprotonated ion at *m/z* 477 $[M-H]^-$. The fragmentation spectra displayed the same predominant ions at *m/z* 313, 295, 169, 163, and 125, characteristic for coumaroyl-*O*-galloyl-hexoside (Hofmann *et al*., 2016). Compound **13** (Rt = 33.56 minutes) exhibited molecular ion peak [*m/z* 787 $(M-H)^-$], the other fragments were at *m/z* 635 [M-152 (gallic unit)-$H]^-$, 617, 477, 313, and 169, and this fragmentation pathway typically matched with tetragalloyl glucose. In addition, compound **17** (Rt

**Table 2.** Tentative identification of chemical constituents of *S. molle* MeOH ext., *n*-BuOH fr. and aqueous part by LC-ESI-MS.

| Comp. No. | Rt (Minute) | MW | $[M-H]^-$ *m/z* | MS fragments | Assigned identification | Sources |
|---|---|---|---|---|---|---|
| 1 | 2.92 | 392 | 391 | 195 (100%) | Hydroxytyrosol acetate dimer | BuOH fr. |
| 2 | 3.00 | 358 | 357 | 195 (100%) | Hydroxytyrosol acetate-*O*-hexoside | BuOH fr. |
| 3 | 5.84 | 332 | 331 | 169 (100%), 125, 79 | Galloyl-*O*-hexoside | MeOH ext. |
| 4 | 8.09 | 170 | 169 | 125 (100%), 79 | Gallic acid[a] | MeOH ext. |
| 5 | 15.78 | 326 | 325 | 169, 125, 79 | Galloylshikimic acid | MeOH ext., BuOH fr. |
| 6 | 16.78 | 326 | 325 | 169, 125, 79 | Galloylshikimic acid isomer | MeOH ext, BuOH fr. |
| 7 | 17.61 | 412 | 411 | 241, 169, 125, 79 | Gallic acid derivatives | BuOH fr. |
| 8 | 21.20 | 184 | 183 | 169, 125, 79 | Methyl gallate | MeOH ext., BuOH fr. |
| 9 | 27.80 | 478 | 477 | 325, 169 (100%), 125, 79 | Digalloyl Shikimic acid | MeOH ext., BuOH fr. |
| 10 | 28.89 | 478 | 477 | 325, 169 (100%), 125, 79 | Digalloyl Shikimic acid isomer | MeOH ext., BuOH fr. |
| 11 | 32.98 | 478 | 477 | 313, 295, 169, 163, 125 | Coumaroyl-*O*- galloyl-hexoside | MeOH ext. |
| 12 | 33.06 | 478 | 477 | 313, 295, 169, 163, 125 | Coumaroyl-*O*- galloyl- hexoside isomer | MeOH ext. |
| 13 | 33.56 | 788 | 787 | 635, 617, 477, 313, 169 | Tetra galloyl glucose | MeOH ext. |
| 14 | 34.65 | 596 | 595 | 301 (100%), 179 | Quercetin-3 *O*- hexoside-pentoside | MeOH ext. |
| 15 | 34.81 | 630 | 629 | 477, 289, 169 (100%), 79 | Gallic acid derivative | MeOH ext. |
| 16 | 35.48 | 616 | 615 | 463, 301, 151 | Quercetin -3-*O*- galloyl- glucose[a] | MeOH ext. |
| 17 | 37.49 | 940 | 939 | 769, 483, 169 (100%), 125, 79 | Penta galloyl glucose | MeOH ext., BuOH fr. |
| 18 | 37.82 | 464 | 463 | 301 (100%) | Quercetin-3-O- glucose[a] | BuOH fr. |
| 19 | 38.32 | 600 | 599 | 463, 301 (100%) | Quercetin-3-*O*- hexoside- protocatechoic acid | MeOH ext. |
| 20 | 39.07 | 478 | 477 | 301 (100%), 151 | Quercetin-3-*O*- hexuronic acid | BuOH fr. |
| 21 | 40.74 | 448 | 447 | 285 (100%) | Kaempferol-3-O- hexoside | MeOH ext. |
| 22 | 41.83 | 448 | 447 | 301 (100%) | Quercetin-3-*O*- rhamnose[a] | MeOH ext. |
| 23 | 42.33 | 462 | 461 | 301, 169 | Quercetin derivatives | MeOH ext. |
| 24 | 42.75 | 484 | 483 | 285 (100%), 151 | Kaempferol derivatives | MeOH ext. |
| 25 | 50.10 | 302 | 301 | 179, 151, 79 | Quercetin[a] | MeOH ext. |
| 26 | 50.43 | 284 | 283 | 268 (100%), 151 | Apigenin-7-*O*- methyl ether | BuOH fr. |
| 27 | 50.93 | 488 | 487 | 283, 268 (100%) | Apigenin-7-*O*- methyl ether- acetyl hexoside | BuOH fr. |
| 28 | 53.69 | 534 | 533 | 387, 301 (100%), 79 | Quercetin-3-*O*-malonyl-deoxyhexose | MeOH ext. |
| 29 | 55.77 | 542 | 541 | 415, 389 | Neochamaejasmin B | MeOH ext. aqueous part |
| 30 | 58.78 | 538 | 537 | 375 | Biapigenin | MeOH ext. aqueous part |
| 31 | 61.28 | 538 | 537 | 375 | Biapigenin isomer | MeOH ext., BuOH fr. |

[a]Compounds identified by comparison with standards.

= 37.49 minutes) afforded $[M-H]^-$ at *m/z* 939, corresponding to pentagalloyl glucose (Hofmann *et al*., 2016; Meyers *et al*., 2006).

On the other hand, the MeOH ext. and *n*-BuOH fraction have some flavonoids such as compound **26** (Rt = 50.10 minutes) which exhibited molecular ion signal at *m/z* 301 $[M-H]^-$, and the second-order spectra of this ion peak exhibited the formation of the ion signals at *m/z* 179, 151, and 79 which are characteristics for quercetin aglycon. Compound **14** (Rt = 34.65 minutes) represented a precursor ion at *m/z* 595 $[M-H]^-$ and then afforded a fragment ion at *m/z* 301 $[M-294-H]^-$, which means the neutral loss of hexosyl-pentoside unit. Thus, this compound was characterized as quercetin-3-*O*-hexosyl-pentoside (Simirgiotis *et al*., 2015). Compound **16** (Rt = 35.48 minutes) produced a quasimolecular ion at *m/z* 615 $[M-H]^-$, and other fragments were at *m/z* 463 $[M-152-H]^-$, which reflected the loss of galloyl unit and peak at *m/z* 301 $[M-152-162-H]^-$, attributed to further loss of glucose unit; this compound was assigned as quercetin-3-*O*-galloyl-glucose (Pascale *et al*., 2020). Compound **18** (Rt = 37.82 minutes) produced molecular ion at *m/z* 463 $[M-H]^-$ and ion signal at *m/z* 301$[M-162-H]^-$, attributed to a neutral loss of glucose unit. Therefore, it was assigned as quercetin-3-*O*-glucose. Compound **19** (Rt = 38.32 minutes) gave molecular ion precursor at *m/z* 599 $[M-H]^-$ and yielded fragment signal at *m/z* 463 $[M-136-H]^-$, attributed to a neutral loss of protocatechuic acid unit, *m/z* 301 [M-136-162 (hexose)-H]$^-$, thus confirming that the compound is quercetin-3-*O*-hexoside-protocatechuic acid. Compound **20** (Rt = 39.07 minutes) represented $[M-H]^-$ *m/z* 599 and fragment peak at *m/z* 301 [M-176 (hexuronic acid)-H]$^-$. Thus, compound **20** was assigned as quercetin-3-*O*-hexuronic acid. Compound **22** (Rt = 41.83 minutes) had molecular ion at *m/z* 447 $[M-H]^-$ and main fragment peak at *m/z* 301 [M-146 (deoxyhexose)-H]$^-$. Thus, it was identified as quercetin-3-*O*-rhamnose (Fernández-Poyatos *et al*., 2019). In addition, compound **28** (Rt = 53.69 minutes) had $[M-H]^-$ at *m/z* 533 and other fragments at *m/z* 387 [M-146 (deoxyhexose)-H]$^-$ and fragment at *m/z* 301[M-146 (deoxyhexose)-86 (malonyl unit)-H]$^-$. Hence, compound **28** was

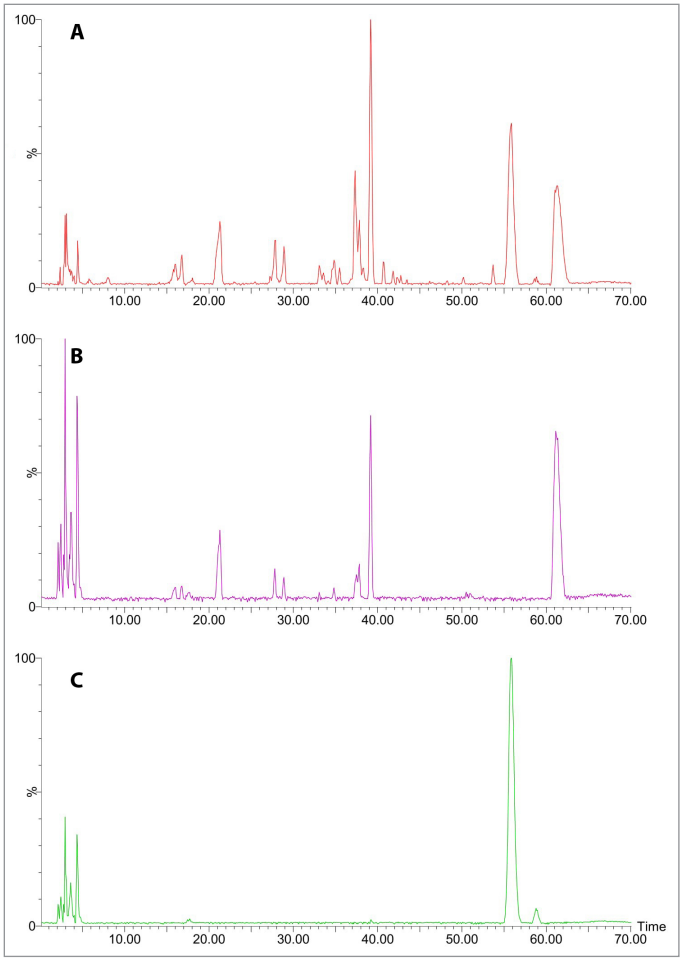


**Figure 4.** LC-ESI-MS base peak chromatograms of MeOH ext. (A), *n*-BuOH fr. (B), and aqueous part (C) of *S. molle* fruits in negative ionization mode.

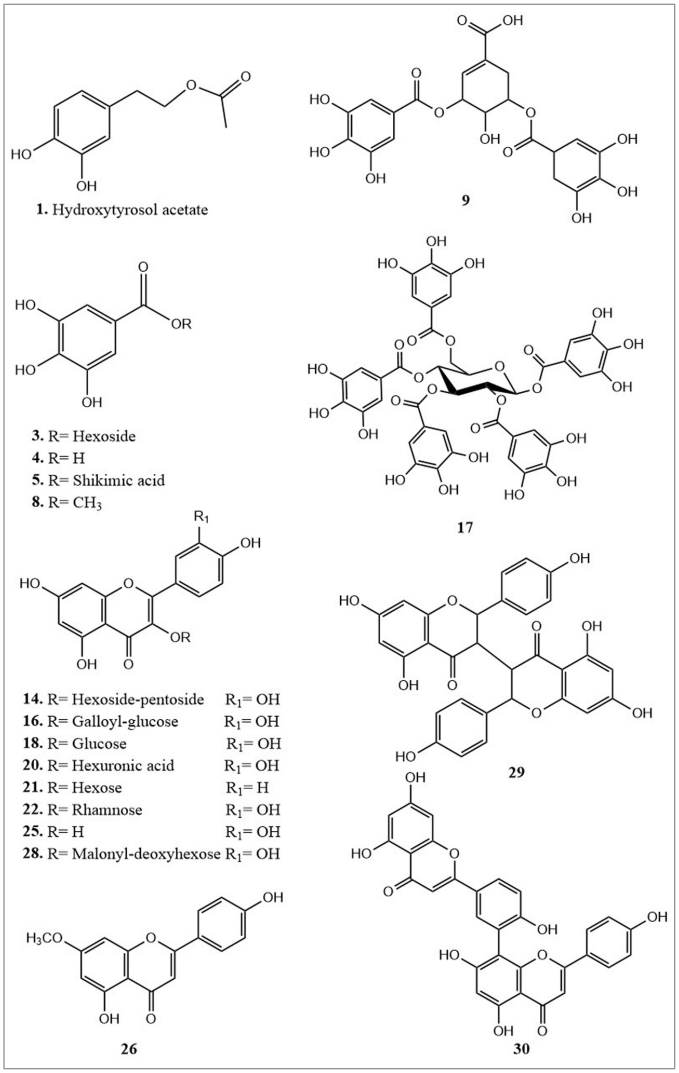


**Figure 5.** Chemical structures of the major compounds identified in *S. molle* extracts by LC-ESI-MS technique.

assigned as quercetin-3-*O*-malonyl-deoxyhexose (Kachlicki *et al*., 2008). Moreover, compound **21** (Rt = 40.74 minutes) had $[M-H]^-$ peak at *m/z* 447 and another signal at *m/z* 285 $[M-162-H]^-$ characteristic for kaempferol aglycone. Thus, it was assigned as kaempferol-3-*O*-hexoside. Compound **24** (Rt = 42.75 minutes) had precursor ions at *m/z* 483 $[M-H]^-$ and *m/z* 285 $[M-198-H]^-$. Therefore, it was assigned as kaempferol derivatives (Chen *et al*., 2015). In addition, compound **26** (Rt = 50.43 minutes) gave precursor ions at *m/z* 283 $[M-H]^-$, and another peak at *m/z* 268 (apigenin) $[M-15-H]^-$ corresponded to the elimination of methyl group; therefore, this compound was assigned as apigenin-7-*O*-methyl ether (Simirgiotis *et al*., 2015), while compound **27** (Rt = 50.93 minutes) represented $[M-H]^-$ at *m/z* 487 and then afforded ion fragments at *m/z* 283 $[M-204-H]^-$ and *m/z* 268 $[M-204-15-H]^-$, attributed to the liberation of acetyl-hexoside and methyl ether units, respectively. Thus, it was assigned as apigenin-7-*O*-methyl ether-acetyl-hexoside (Simirgiotis *et al*., 2015). Compound **29** (Rt = 55.77 minutes) had a molecular ion peak at *m/z* 541 $[M-H]^-$ and afforded other fragments at *m/z* 415 and 389, characteristics for the fragmentation pattern of neochamaejasmin B (Huang *et al*., 2010). Compounds **30** (Rt = 58.78 minutes) and compounds **31** (Rt = 61.28 minutes) represented molecular ion signals at *m/z* 537 $[M-H]^-$ and another fragment at *m/z* 375, characteristics for biapigenin. This compound was isolated before from the fruits of *S. molle* by Ono *et al*. (2008). These results indicated that *S. molle* extracts had various chemical compositions such as flavonoids (apigenin, kaempferol, and quercetin derivatives), phenolic acids, phenylethanoids, and gallotannins. Moreover, Figure 4 showed high abundant peaks identified as methyl gallate, digalloyl shikimic acid, pentagalloyl glucose, quercetin-3-*O*-glucose, quercetin-3-*O*-hexuronic acid, neochamaejasmin B, and biapigenin. These active ingredients may be responsible for the potent anticancer activity of *S. molle* fruit extracts. Moreover, the chemical profiling of *n*-BuOH fraction represented a high content of flavonoids, phenolic acids, phenylethanoids, and gallotannins which may be responsible for its high cytotoxic potential.

## CONCLUSION

In the present study, *S. molle* fruit extracts possessed a promising cytotoxic potential against the HepG-2 cell line. The chemical investigation of the volatile constituents of *n*-hexane

ext. and the essential oil using GC-MS analysis led to identifying 50 compounds classified as monoterpenes, sesquiterpenes, and fatty acids, while the LC-ESI-MS chemical investigation of the 85% MeOH ext., *n*-BuOH fraction, and aqueous part led to characterize 31 polyphenolic compounds, for example, phenolic acids, flavonoids, phenylethanoids, and gallotannins. From the available literature, these bioactive secondary metabolites (volatile and nonvolatile constituents) had a broad spectrum of biological and pharmacological properties. Thus, our results suggested the selective potential of tested extracts for the treatment of different types of cancer and the possible usage of *S. molle* extracts as anticancer therapeutic agents.

## LIST OF ABBREVIATIONS

| | |
|---|---|
| GC-MS | Gas chromatography-mass spectrometry |
| IC | Inhibition concentration |
| LC-ESI-MS | Liquid chromatography-electron spray ionization-mass spectrometry |
| MeOH ext. | Methanol extract |
| *n*-BuOH | Normal-butanol |
| *n*-hexane | Normal-hexane |
| SRB | Sulforhodamine B |

## ETHICAL APPROVAL

The present work does not include the use of human or animal subjects.

## CONFLICT OF INTEREST

The authors declare that there are no conflicts of interest.

## FUNDING

None.

## PUBLISHER'S NOTE

This journal remains neutral with regard to jurisdictional claims in published institutional affiliation.

## REFERENCES

Abdel-Hameed ES, Bazaid SA. Chemical composition of essential oil from leaves of *Schinus molle* L. Growing in Taif, KSA. J Essent Oil Bear Pl, 2017; 20(1):45–58.

Abdel-Hamid NM, Abass SA, Mohamed AA, Hamid DM. Herbal management of hepatocellular carcinoma through cutting the pathways of the common risk factors. Biomed Pharmacother, 2018; 107:1246–58.

Abdel-Sattar E, Zaitoun AA, Farag MA, El Gayed SH, Harraz FM. Chemical composition, insecticidal and insect repellent activity of *Schinus molle* L. leaf and fruit essential oils against *Trogoderma granarium* and *Tribolium castaneum*. Nat Prod Res, 2010; 24:226–35.

Anyasor GN, Idowu DP, Nabofa W. Evaluation of the hepatoprotective effect of oral administration of aqueous fraction of methanolic extract of *Costus afer* leaves during induction of hepatocellular carcinoma with diethylnitrosamine in rats. Comp Clin Path, 2020; 29:733–44.

Bray F, Ferlay J, Soerjomataram I, Siegel RL, Torre LA, Jemal A. Global cancer statistics 2018: GLOBOCAN estimates of incidence andmortality worldwide for 36 cancers in 185 countries. CA Cancer J Clin, 2018; 68:1–31.

Cavalcanti AS, Alves MS, Silva LCP, Patrocínio DS, Sanches MN, Chaves DSA, Souza MAA. Volatiles composition and extraction kinetics from *Schinus terebinthifolius* and *Schinus molle* leaves and fruit. Rev Bras Farmacogn, 2015; 25:356–62.

Chedid F, Kruel C, Pinto M, Grezzan-filho T, Ian L. Hepatocellular carcinoma: diagnosis and operative management. Arq Bras Cir Dig, 2017; 30:272–8.

Chen, Y, Yu H, Wu H, Pan Y, Wang K, Jin Y, Zhang C. 2015. Characterization and quantification by LC-MS/MS of the chemical components of the heating products of the flavonoids extract in pollen typhae for transformation rule exploration. Molecules, 2015; 20:18352–66.

Escobar-Avello D, Lozano-Castellón J, Mardones C, Pérez AJS, Vania RS, von Baer D, Vallverdú-Queralt A. Phenolic profile of grape canes: novel compounds identified by LC-ESI-LTQ-Orbitrap-MS. Molecules, 2019; 24:3763.

Fernández-Poyatos MP, Ruiz-Medina A, Zengin G, Llorent-Martínez EJ. Phenolic characterization, antioxidant activity, and enzyme inhibitory properties of *Berberis thunbergii* DC. Leaves: a valuable source of phenolic acids. Molecules, 2019; 24:4171.

Garzoli S, Masci VL, Ovidi E, Turchetti G, Zago D, Tiezzi A. Chemical Investigation of a biologically active *Schinus molle* L. leaf extract. J Anal Methods Chem, 2019; 2019:1–6.

Geran RI, Greenberg NH, Macdonald MM, Schumacher AM, Abbott BJ. Protocols for screening chemical agents and natural products against animal tumors and other biological systems. Cancer Chemother Rep, 1972; 3:1–103.

Gomes V, Agostini G, Agostini F, Atti dos Santos AC, Rossato M. Variation in the essential oils composition in Brazilian populations of *Schinus molle* L. (Anacardiaceae). Biochem Syst Ecol, 2013; 48:222–7.

Hamdan DI, Al-Gendy AA, El-Shazly AM. Chemical composition and cytotoxic activity of the essential oils of *Schinus molle* growing in Egypt. J Pharm Sci Res, 2016; 8(8):779–93.

Hayouni E, Chraief I, Abedrabba M, Bouix M, Leveau JY, Mohammed H, Hamdi M. Tunisian *Salvia officinalis* L. and *Schinus molle* L. essential oils: Their chemical compositions and their preservative effects against Salmonella inoculated in minced beef meat. Int Food Microbiol, 2008; 125:242–51.

Hofmann T, Nebehaj E, Albert L. Antioxidant properties and detailed polyphenol profiling of European hornbeam (*Carpinus betulus* L.) leaves by multiple antioxidant capacity assays and high-performance liquid chromatography/multistage electrospray mass spectrometry. Ind Crops Prod, 2016; 87:340–9.

Hosni K, Jemli M, Dziri S, Mrabet Y, Ennigrou A, Sghaier A, Casabianca H, Vulliet EBN, Sebei H. Changes in phytochemical, antimicrobial and free radical scavenging activities of the peruvian pepper tree (*Schinus molle* L.) as influenced by fruit maturation. Ind Crops Prod, 2011; 34:1622–8.

Huang Q, Chen H, Ren Y, Wang Z, Zeng P, Li X, Wang J, Zheng X. Anti-hepatocellular carcinoma activity and mechanism of chemopreventive compounds: ursolic acid derivatives. Pharm Biol, 2016; 54(12):3189–96.

Huang W, Zhang X, Wang Y, Ye W, Ooi VEC, Chung HY, Li Y. Antiviral biflavonoids from *Radix Wikstroemiae* (Liaogewanggen). Chin Med, 2010; 5(23):1–6.

Kachlicki P, Einhorn J, Muth D, Kerhoas L, Stobiecki M. Evaluation of glycosylation and malonylation patterns in flavonoid glycosides during LC/MS/MS metabolite profiling. J Mass Spectrom, 2008; 43:572–86.

Khlifi D, Hayouni E, Valentin A, Cazaux S, Moukarzel B, Hamdi M, Bouajil J. LC–MS analysis, anticancer, antioxidant and antimalarial activities of *Cynodon dactylon* L. extracts. Indust Crops Prod, 2013; 45:240–7.

Li C, Seeram NP. Ultra-fast liquid chromatography coupled with electrospray ionization/time-of- flight mass spectrometry for rapid phenolic profiling of red maple (*Acer rubrum*) leaves. J Sep Sci, 2018; 41(11):2331–46.

López A, Castro S, Andina MJ, Ures X, Munguía B, Llabot JM, Elder H, Dellacassa E, Palma S, Domínguez L. Insecticidal activity of microencapsulated *Schinus molle* essential oil. Ind Crops Prod, 2014; 53:209–16.

Machado CD, Raman V, Rehman JU, Maia BHLNS, Meneghetti EK, Almeida VP, Silva RZ, Farago PV, Khan IA, Budel JM. *Schinus molle*: anatomy of leaves and stems, chemical composition and insecticidal activities of volatile oil against bed bug (*Cimex lectularius*). Rev Bras Farmacgn, 2019; 29:1–10.

Malca-García GR, Hennig L, Ganoza-Yupanqui ML, Pina-Iturbe A, Bussmann RW. Constituents from the bark resin of *Schinus molle*. Rev Bras Farmacogn, 2017; 27:67–9.

Martins MR, Arantes S, Candeias F, Tinoco MT, Cruz-Morais J. Antioxidant, antimicrobial and toxicological properties of *Schinus molle* L. essential oils. J Ethnopharmacol, 2014; 15:485–92.

Mena P, Calani L, Dall'Asta C, Galaverna G, García-Viguera C, Bruni R, Crozier A, Del RD, Rapid and comprehensive evaluation of (Poly)phenolic compounds in pomegranate (*Punica granatum* L.) juice by UHPLC-MS$^n$. Molecules, 2012; 17:14821–40.

Meyers KJ, Swiecki TJ, Mitchell AE. Understanding the native Californian diet: identification of condensed and hydrolyzable tannins in Tanoak Acorns (*Lithocarpus densiflorus*). J Agric Food Chem, 2006; 54:7686–91.

Nguyen NH, Ta QTH, Pham QT, Luong TNH, Phung VT, Duong TH, Vo VG, Anticancer activity of novel plant extracts and compounds from *Adenosma bracteosum* (Bonati) in human lung and liver cancer cells. Molecules, 2020; 25:2912.

Ono M, Yamashita M, Mori K, Masuoka C, Eto M, Kinjo J, Ikeda T, Yoshimitsu H, Nohara T. Sesquiterpenoids, triterpenoids, and flavonoids from the fruits of *Schinus molle*. Food Sci Technol Res, 2008; 14(5):499–508.

Pascale R, Acquavia MA, Cataldi TRI, Onzo A, Coviello D, Bufo SA, Scrano L, Ciriello R, Guerrieri A, Bianco G. Profiling of quercetin glycosides and acyl glycosides in sun-dried peperoni di Senise peppers (*Capsicum annuum* L.) by a combination of LC-ESI (-)-MS/MS and polarity prediction in reversed-phase separations. Anal Bioanal Chem, 2020; 412:3005–15.

Shahat AA, Hidayathulla S, Khan AA, Alanazi AM, Al Meanazel OT, Alqahtani AS, Alsaid MS, Hussein AA. Phytochemical profiling, antioxidant and anticancer activities of *Gastrocotyle hispida* growing in Saudi Arabia. Acta Trop, 2019; 191:243–7.

Siddiqui S, Ahmad R, Khan MA, Upadhyay S, Husain I, Srivastava AN. Cytostatic and anti-tumor potential of Ajwa date pulp against human hepatocellular carcinoma HepG2 cells. Sci Rep, 2019; 9:245.

Simionatto E, Chagas MO, Peres MTLP, Hess SC, Silva CB, Ré-Poppi N, Gebara SS, Corsino J, Morel AF, Stuker CZ, Matos MFC, Carvalho JE.. Chemical composition and biological activities of leaves essential oil from *Schinus molle* (Anacardiaceae). J Essent Oil Bear Pl, 2011; 14:590–9.

Simirgiotis MJ, Benites J, Areche C, Sepúlveda B. Antioxidant capacities and analysis of phenolic compounds in three endemic *Nolana* species by HPLC-PDA-ESI-MS. Molecules, 2015; 20:11490–507.

Singh SK, Patra A. Evaluation of phenolic composition, antioxidant, anti-inflammatory and anticancer activities of *Polygonatum verticillatum* (L.). J Integr Med, 2018; 16:273–82.

Skehan PR, Storeng D, Scudiero. New colorimetric cytotoxicity assay for anticancer drug screening. J Natl Cancer Inst, 1990; 82(13):1107–12.

Tasioula-Margari M, Tsabolatidou E. Extraction, separation, and identification of phenolic compounds in virgin olive oil by HPLC-DAD and HPLC-MS. Antioxidants, 2015; 4:548–62.

Vichai V, Kirtikara K. Sulforhodamine B colorimetric assay for cytotoxicity screening. Nat Protoc, 2016; 1(3):1112–6.

Wyrepkowski CC, Gomes CD, Lu M, Sinhorin AP, Vilegas W, De Grandis RA, Resende FA, Varanda EA, Campaner SL. Characterization and Quantification of the compounds of the ethanolic extract from *Caesalpinia ferrea* stem bark and evaluation of their mutagenic activity. Molecules, 2014; 19:16039–57.

**How to cite this article:**
Osman EEA, Morsi EA, El-Sayed MM, Gobouri A, Abdel-Hameed ES. Identification of the volatile and nonvolatile constituents of *Schinus molle* (L.) fruit extracts and estimation of their activities as anticancer agents. J Appl Pharm Sci, 2021; 11(07):163–171.